International Journal of Mechanical Sciences 51 (2009) 508–514

Contents lists available at ScienceDirect

International Journal of Mechanical Sciences

journal homepage: www.elsevier.com/locate/ijmecsci

Static and kinematic limit analysis of orthotropic strain-hardening pressure vessels involving large deformation

S.-Y. Leu *

Department of Aviation Mechanical Engineering, China Institute of Technology, No. 200, Jhonghua St., Hengshan Township, Hsinchu County 312, Taiwan, ROC

ARTICLE INFO

Article history:
Received 10 February 2009
Received in revised form
30 April 2009
Accepted 15 May 2009
Available online 23 May 2009

Keywords:
Limit analysis
Large deformation
Sequential limit analysis
Thick-walled cylindrical vessel
Voce hardening law
Hill's yield criterion

ABSTRACT

This paper analytically investigates plastic limit pressure of orthotropic strain-hardening cylindrical vessels under internal pressure. It is an interesting problem to illustrate the interaction between strengthening and weakening behavior during the deformation process. The Voce hardening law and Hill's yield criterion were adopted in the paper. A sequence of static and kinematic limit analysis problems were performed by updating the yield criterion and the deformed configuration. The equality relation between the greatest lower bound and the least upper bound was confirmed explicitly. Accordingly, exact solutions of plastic limit pressure were developed with an integral term. Particularly, exact closed-form solutions were obtained for certain values of the hardening exponent of the Voce hardening law. Finally, numerical efforts were also made for rigorous validations.

1. Introduction

Internally pressurized cylinders of perfectly plastic isotropic materials have been well studied, e.g. [1]. On the other hand, attention has been also paid to the effect of plastic anisotropy on the limit pressure for perfectly plastic materials, e.g. [2,3]. Recently, Güven [4] investigated failure pressures of cylindrical pressure vessels made of transversely isotropic materials considering the Voce hardening law [5].

As is well known, limit analysis can directly provide the plastic limit load for optimal structure design and safety evaluation by the static or the kinematic theorem [6]. By the kinematic theorem of limit analysis, Jiang [7] and Capsoni et al. [3] provided analytical solutions of limit pressure of plane-strain axi-symmetric tubes made of perfectly plastic materials based on the von Mises and Hill's yield criteria [8], respectively. On the other hand, if we consider structures made of strain-hardening materials, it is appropriate to evaluate the load-bearing capacity by limit analysis sequentially [9–13]. Further, the author applied sequential limit analysis to illustrate the interesting interaction between strengthening and weakening behavior during the deformation process involving strain-hardening materials [14–18]. Actually, sequential limit analysis has been illustrated extensively [9–23] to be an accurate and efficient tool for the large-deformation analysis. By sequential limit analysis, it is possible to conduct a sequence of limit analysis problems by updating the yield criterion and the deformed configuration [19]. Accordingly, rigorous lower-bound or upper-bound solutions are then acquired sequentially to approach the real limit solutions in the whole deforming process.

This paper is aimed to apply the concept of sequential limit analysis to analytically investigate plastic limit pressure of axi-symmetric plane-strain cylinders considering the Voce hardening law [5] and the effects of plastic anisotropy. Analytical efforts of both static and kinematic limit analysis are to be made for plastically orthotropic materials, namely transversely isotropic materials and planar anisotropic materials. On the one hand, we seek the greatest lower bound of limit pressure by static limit analysis [6]. On the other hand, we search for the least upper bound of limit pressure by kinematic limit analysis [6]. Theoretically, the equality relation between the greatest lower bound and the least upper bound can be established by duality theorems [6,19,24]. Accordingly, we can obtain the exact limit pressure by confirming the equality relation between the greatest lower bound and the least upper bound of limit pressure.

2. Analytical background

We analytically derive plastic limit pressure of orthotropic thick-walled hollow cylinders made of materials with nonlinear isotropic hardening subjected to internal pressure in plane-strain conditions. The behavior of nonlinear isotropic hardening is

* Tel.: +886 3 5935707; fax: +886 3 5936297.
E-mail address: syleu@cc.chit.edu.tw

0020-7403/$ - see front matter © 2009 Elsevier Ltd. All rights reserved.
doi:10.1016/j.ijmecsci.2009.05.004

Nomenclature

a_0	initial interior radius
a	current interior radius
$\dot{a}$	velocity of the current interior radius
b_0	initial exterior radius
b	current exterior radius
D	problem domain
∂D_s	static boundary
∂D_k	kinematic boundary
F	anisotropy coefficient of Hill's yield criterion
G	anisotropy coefficient of Hill's yield criterion
H	anisotropy coefficient of Hill's yield criterion
h	hardening exponent of the Voce hardening law
$\hat{h}$	notation related to the hardening exponent and plastic anisotropy parameters
$\vec{n}$	unit outward normal vector of a boundary
P	plastic anisotropy parameter
P_i	internal pressure
q	load factor
$q(\sigma)$	lower-bound functional
$\bar{q}(\vec{u})$	upper-bound functional
q^*	exact limit solution
R	plastic anisotropy parameter
R_{11}	anisotropic yield stress ratio
R_{22}	anisotropic yield stress ratio
R_{33}	anisotropic yield stress ratio
r_0	initial radius of the location concerned
r	current radius of the location concerned
$\underrightarrow{S}$	length of the innermost edge
$\vec{t}$	scalable distribution of a traction vector
u_r	radial velocity
$\vec{u}$	velocity field
$\|\sigma\|_H$	Hill's yield criterion primal norm on stress tensor
$\|\dot{\varepsilon}\|_{-H}$	Hill's yield criterion dual norm on strain rate tensor
σ	stress tensor
σ_r	radial stress
σ_Y	yield strength
σ_0	initial yield strength
σ_∞	saturation value of yield strength
$\bar{\sigma}$	equivalent stress
$\bar{\varepsilon}$	equivalent strain
$\dot{\varepsilon}$	strain rate tensor
$\dot{\varepsilon}_r$	radial strain rate
$\dot{\varepsilon}_\theta$	circumferential strain rate
$\dot{\bar{\varepsilon}}$	equivalent strain rate
∇	del operator (or Nabla operator)

described by the Voce hardening law [5]

$$\sigma_Y = \sigma_\infty - (\sigma_\infty - \sigma_0)\exp(-h\bar{\varepsilon}) \tag{1}$$

where σ_Y is the yield strength, σ_0 the initial yield strength, σ_∞ the saturation value of σ_0, h the hardening exponent and $\bar{\varepsilon}$ the equivalent strain.

The thick-walled cylindrical vessel concerned has the initial interior and exterior radii indicated by a_0 and b_0, respectively. After the action of internal pressure, its current interior and exterior radii are denoted by a and b in the induced widening process, respectively. In addition, we consider a thick-walled cylindrical vessel under internal pressure with the boundary conditions $\sigma_r(r=a)=P_i$ and $\sigma_r(r=b)=0$ with P_i the value of internal pressure and r the current radius.

In the following derivations, the behavior of plastic orthotropy is simulated by utilizing Hill's yield criterion [8]. Particularly, the principal axes of orthotropy are assumed to form an orthogonal set coinciding with the cylindrical co-ordinates of the cylinder. Therefore, we can simplify the problem concerned into an axi-symmetric plane-strain problem. Accordingly, the yield function is reduced to the form as

$$F(\sigma_\theta-\sigma_z)^2 + G(\sigma_z-\sigma_r)^2 + H(\sigma_r-\sigma_\theta)^2 = 1 \tag{2}$$

where F, G and H are parameters defined as [8]

$$F = \frac{1}{2}\left(\frac{1}{R_{22}^2}+\frac{1}{R_{33}^2}-\frac{1}{R_{11}^2}\right) \tag{3}$$

$$G = \frac{1}{2}\left(\frac{1}{R_{33}^2}+\frac{1}{R_{11}^2}-\frac{1}{R_{22}^2}\right) \tag{4}$$

$$H = \frac{1}{2}\left(\frac{1}{R_{11}^2}+\frac{1}{R_{22}^2}-\frac{1}{R_{33}^2}\right) \tag{5}$$

where R_{11}, R_{22} and R_{33} are anisotropic yield stress ratios. According to the work of Liu et al. [25], the yield function is convex if we have

$$(F+H)(G+H)-H^2 \geq 0 \tag{6}$$

Equivalently, we have

$$\frac{R_{11}R_{22}}{R_{11}+R_{22}} \leq R_{33} \leq \frac{R_{11}R_{22}}{|R_{11}-R_{22}|} \tag{7}$$

Further, corresponding to Hill's yield criterion [8] with the associated flow rule, we have the equivalent stress $\bar{\sigma}$ and the equivalent strain rate $\dot{\bar{\varepsilon}}$ as follows [8,26]:

$$\bar{\sigma} = \sqrt{\frac{R}{P(R+1)}(\sigma_\theta-\sigma_z)^2 + \frac{1}{R+1}(\sigma_z-\sigma_r)^2 + \frac{R}{R+1}(\sigma_r-\sigma_\theta)^2} \tag{8}$$

$$\dot{\bar{\varepsilon}} = \sqrt{\frac{P(R+1)}{R(P+R+1)^2}(\dot{\varepsilon}_\theta - R\dot{\varepsilon}_z)^2 + \frac{R+1}{(P+R+1)^2}(P\dot{\varepsilon}_z-\dot{\varepsilon}_r)^2 + \frac{R+1}{R(P+R+1)^2}(R\dot{\varepsilon}_r - P\dot{\varepsilon}_\theta)^2} \tag{9}$$

where we have the plastic anisotropy parameters $R=H/G$ and $P=H/F$.

Considering plane-strain conditions and incompressibility, we can further reduce the equivalent stress $\bar{\sigma}$ and the equivalent strain rate $\dot{\bar{\varepsilon}}$ into the following simplified forms:

$$\bar{\sigma} = \sqrt{\frac{R(P+R+1)}{(P+R)(R+1)}}(\sigma_\theta-\sigma_r) \tag{10}$$

$$\dot{\bar{\varepsilon}} = \sqrt{\frac{(P+R)(R+1)}{R(P+R+1)}}\dot{\varepsilon}_\theta \tag{11}$$

On the other hand, due to axi-symmetry, the strain rate–velocity relations are given by

$$\dot{\varepsilon}_r = \frac{du_r}{dr} \tag{12}$$

$$\dot{\varepsilon}_\theta = \frac{u_r}{r} \tag{13}$$

where $\dot{\varepsilon}_r$ and $\dot{\varepsilon}_\theta$ are the radial and circumferential strain rates, respectively, and u_r is the velocity component in the radial direction. Also, we have the incompressibility in plane-strain

conditions described in the form

$$\nabla \cdot \vec{u} = \dot{\varepsilon}_r + \dot{\varepsilon}_\theta = 0 \tag{14}$$

where ∇ is the del operator (or Nabla operator). To meet the incompressibility in plane-strain conditions, we have the radial velocity indicated in the form

$$u_r = \frac{a\dot{a}}{r} \tag{15}$$

where $\dot{a}$ is the velocity of the current interior radius.

Accordingly, we rewrite the equivalent strain rate $\dot{\bar{\varepsilon}}$ in the form

$$\dot{\bar{\varepsilon}} = \sqrt{\frac{(P+R)(R+1)}{R(P+R+1)}}\frac{a\dot{a}}{r^2} \tag{16}$$

The equivalent strain is then obtained as

$$\bar{\varepsilon} = \int \dot{\bar{\varepsilon}}\, dt = \frac{1}{2}\sqrt{\frac{(P+R)(R+1)}{R(P+R+1)}}\ln\frac{r^2}{r_0^2} \tag{17}$$

where r_0 is the initial radius of the location concerned.

Combining Eqs. (1) and (17), the Voce hardening law [5] can be rewritten in the form as

$$\sigma_Y = \sigma_\infty - (\sigma_\infty - \sigma_0)\frac{r_0^{2\hat{h}}}{r^{2\hat{h}}} \tag{18}$$

where the notation $\hat{h}$ is indicated as

$$\hat{h} = \frac{h}{2}\sqrt{\frac{(P+R)(R+1)}{R(P+R+1)}} \tag{19}$$

3. Static and kinematic limit analysis

3.1. Static limit analysis

We consider a general plane-strain problem with the domain D consisting of the static boundary ∂D_s and the kinematic boundary ∂D_k [24]. Based on the concept of sequential limit analysis, the quasi-static problem is to seek the maximum allowable driving load sequentially under constraints of static and constitutive admissibility such that

$$\begin{array}{lll} \text{maximize} & q(\sigma) & \\ \text{subject to} & \nabla\cdot\sigma = 0 & \text{in } D \\ & \sigma\cdot\vec{n} = q\,\vec{t} & \text{on } \partial D_S \\ & \|\sigma\|_H \le \sigma_Y & \text{in } D \end{array} \tag{20}$$

where $\vec{n}$ indicates the unit outward normal vector of the boundary and the traction vector $\vec{t}$ is a scalable distribution of the driving load on ∂D_s with the load factor q; $\|\sigma\|_H$ means the primal norm [6] of Hill's yield criterion on stress tensor σ. Therefore, this constrained problem is to sequentially maximize the load factor q representing the magnitude of the driving load for each step.

The primal problem Eq. (20) is the lower-bound formulation seeking the maximum solution under constraints of static and constitutive admissibilities. The statically admissible solutions satisfy the equilibrium equation and the static boundary condition. The constitutive admissibility is stated by the yield criterion in an inequality form. We can interpret the solutions as sets as shown in the work of Huh and Yang [6] and Yang [19]. First, the equilibrium equation is linear and the constitutive inequality is convex and bounded. Accordingly, the intersection of statically admissible set and constitutively admissible set is convex and bounded. Moreover, the existence of a unique maximum to the convex programming problem is confirmed.

To seek the greatest lower bound, we substitute Eqs. (10) and (18) into the following equilibrium equation:

$$\nabla\cdot\sigma = \frac{\partial\sigma_r}{\partial r} + \frac{\sigma_r - \sigma_\theta}{r} = 0 \tag{21}$$

such that

$$\frac{\partial\sigma_r}{\partial r} = \frac{1}{r}\sqrt{\frac{(P+R)(R+1)}{R(P+R+1)}}\left[\sigma_\infty - (\sigma_\infty - \sigma_0)\frac{r_0^{2\hat{h}}}{r^{2\hat{h}}}\right] \tag{22}$$

After some manipulation, we can obtain the greatest lower bound of plastic limit pressure in the form as

$$\begin{aligned} \frac{\sigma_r(r=a)}{\sigma_0} &= \frac{P_i}{\sigma_0} \\ &= -\frac{1}{2}\sqrt{\frac{(P+R)(R+1)}{R(P+R+1)}} \\ &\quad\times\left\{\frac{\sigma_\infty}{\sigma_0}\ln\frac{b^2}{a^2} - 2(\sigma_\infty/\sigma_0 - 1)\int_a^b \frac{(a_0^2 - a^2 + r^2)^{\hat{h}}}{r^{2\hat{h}+1}}dr\right\} \end{aligned} \tag{23}$$

Note that, the sign convention for the internal pressure P_i is positive for tension and negative for compression. Accordingly, the load factor q is obtained as the following form:

$$\begin{aligned} \frac{q}{\sigma_0} &= \frac{1}{2}\sqrt{\frac{(P+R)(R+1)}{R(P+R+1)}} \\ &\quad\times\left\{\frac{\sigma_\infty}{\sigma_0}\ln\frac{b^2}{a^2} - 2(\sigma_\infty/\sigma_0 - 1)\int_a^b \frac{(a_0^2 - a^2 + r^2)^{\hat{h}}}{r^{2\hat{h}+1}}dr\right\} \end{aligned} \tag{24}$$

3.2. Kinematic limit analysis

Now we intend to transform the lower-bound formulation to the upper-bound formulation, similar to the previous work of Huh and Yang [6]. Equilibrium equations can be restated weakly in the form as

$$\int_D \vec{u}\cdot(\nabla\cdot\sigma)\, dA = 0 \tag{25}$$

where $\vec{u}$ is a kinematically admissible velocity field. Integrating by parts, using the divergence theorem and imposing static boundary conditions, we may rewrite Eq. (25) to give an expression for $q(\sigma)$ as

$$\int_{\partial D_s}\vec{u}\cdot q\,\vec{t}\; dS = q\int_{\partial D_s}\vec{u}\cdot\vec{t}\; dS = \int_D \sigma : \dot{\varepsilon}\, dA \tag{26}$$

where $\dot{\varepsilon}$ is the strain rate tensor.

Since the power $\sigma : \dot{\varepsilon}$ is nonnegative, it is clear that $\sigma : \dot{\varepsilon} = |\sigma : \dot{\varepsilon}|$. Further, according to a generalized Hölder inequality [27], and the normality condition in plasticity [28], it results in [10]

$$\sigma : \dot{\varepsilon} = |\sigma : \dot{\varepsilon}| \le \|\sigma\|_H \|\dot{\varepsilon}\|_{-H} = \bar{\sigma}\,\dot{\bar{\varepsilon}} \tag{27}$$

where $\|\dot{\varepsilon}\|_{-H}$ is the dual norm [6] of $\|\sigma\|_H$ based on the flow rule associated with Hill's yield criterion [8]. For the axi-symmetric plane-strain cylinder problem, we have

$$\|\sigma\|_H = \sqrt{\frac{R(P+R+1)}{(P+R)(R+1)}}(\sigma_\theta - \sigma_r) = \bar{\sigma} \tag{28}$$

$$\|\dot{\varepsilon}\|_{-H} = \sqrt{\frac{(P+R)(R+1)}{R(P+R+1)}}\dot{\varepsilon}_\theta = \dot{\bar{\varepsilon}} \tag{29}$$

Combining Eqs. (26) and (27), we have

$$\begin{aligned} q\int_{\partial D_s}\vec{u}\cdot\vec{t}\; dS = \int_D \sigma : \dot{\varepsilon}\, dA &\le \int_D \|\sigma\|_H\|\dot{\varepsilon}\|_{-H}\, dA \\ &\le \int_D \sigma_Y\|\dot{\varepsilon}\|_{-H}\, dA \end{aligned} \tag{30}$$

Since $\vec{u}$ appears homogeneously and linearly in inequality Eq. (30), we can normalize the relationship by setting the following normalization:

$$\int_{\partial D_s} \vec{u}\cdot\vec{t}\ dS = 1 \tag{31}$$

which is to be treated as one of the constraints.

Accordingly, $q(\sigma)$ can be bounded above by $\bar{q}(\vec{u})$ as

$$\begin{aligned} q(\sigma) &= \int_D \sigma : \dot{\varepsilon}\, dA \\ &\le \int_D \|\sigma\|_H \|\dot{\varepsilon}\|_{-H}\, dA \\ &\le \int_D \sigma_Y \|\dot{\varepsilon}\|_{-H}\, dA = \bar{q}(\vec{u}) \end{aligned} \tag{32}$$

Thus, the upper-bound formulation is stated in the form of a constrained minimization problem as

$$\begin{array}{lll} \text{minimize} & \bar{q}(\vec{u}) & \\ \text{subject to} & \bar{q}(\vec{u}) = \int_D \sigma_Y \|\dot{\varepsilon}\|_{-H}\, dA & \\ & \int_{\partial D_s} \vec{u}\cdot\vec{t}\ dS = 1 & \text{on } \partial D_S \\ & \nabla\cdot\vec{u} = 0 & \text{in } D \\ & \text{kinematic boundary conditions on } \partial D_k & \end{array} \tag{33}$$

where $\nabla\cdot\vec{u}=0$ is the incompressibility constraint inherent in Hill's yield criterion [8]. Therefore, the upper-bound formulation seeks sequentially the least upper bound for each step on kinematically admissible solutions.

In the stress control approach, the normalization condition Eq. (31) is based on the simulation of the action of pressure load by imposing a uniform stress (pressure) field [6,9–11,23]. For the case of a circular cylindrical vessel under internal pressure, the traction vector $\vec{t}$, namely the scalable distribution of the driving load with the load factor q, is just a unit vector in the radial direction. Therefore, the normalization condition implies that

$$\int_{\partial D_s} \vec{u}\cdot\vec{t}\ \mathrm{d}S = 2\pi a\dot{a} \tag{34}$$

According to Eqs. (31) and (34), we have

$$2\pi a\dot{a} = 1 \tag{35}$$

Combining Eqs. (16) and (18), the upper-bound functional can be obtained in the form

$$\begin{aligned} \bar{q}(\vec{u}) &= \int_D \sigma_Y \|\dot{\varepsilon}\|_{-\mathrm{H}}\, dA \\ &= \sqrt{\frac{(P+R)(R+1)}{R(P+R+1)}} \\ &\quad\times \int_D \left(\sigma_\infty - (\sigma_\infty-\sigma_0)\frac{r_0^{2\hat{h}}}{r^{2\hat{h}}}\right)\frac{a\dot{a}}{r^2} r\, dr\, d\theta \\ &= 2\pi a\dot{a}\sqrt{\frac{(P+R)(R+1)}{R(P+R+1)}} \\ &\quad\times \left(\frac{\sigma_\infty}{2}\ln\frac{b^2}{a^2} - (\sigma_\infty-\sigma_0)\int_a^b \frac{r_0^{2\hat{h}}}{r^{2\hat{h}+1}}\, dr\right) \end{aligned} \tag{36}$$

According to Eqs. (35) and (36), we have the least upper bound of plastic limit pressure in the form

$$\begin{aligned} \frac{\bar{q}}{\sigma_0} &= \frac{1}{2}\sqrt{\frac{(P+R)(R+1)}{R(P+R+1)}} \\ &\quad\times \left(\frac{\sigma_\infty}{\sigma_0}\ln\frac{b^2}{a^2} - 2(\sigma_\infty/\sigma_0-1)\int_a^b \frac{(a_0^2-a^2+r^2)^{\hat{h}}}{r^{2\hat{h}+1}}\, dr\right) \end{aligned} \tag{37}$$

4. Exact limit solution

The primal–dual problems Eqs. (20) and (33) are convex programming problems [6,19]. Thus, there exists a unique maximum and a minimum to problems Eqs. (20) and (33), respectively. Accordingly, the extreme values of the lower-bound functional $q(\sigma)$ and its corresponding upper-bound functional $\bar{q}(\vec{u})$ are equal to the unique, exact solution q^* for each step in a process. Namely

$$\text{maximize } q(\sigma) = q^* = \text{minimize } \bar{q}(\vec{u}) \tag{38}$$

As shown in the derivations, the greatest lower bound Eq. (24) equals the least upper bound Eq. (37). Namely, we have the exact solution of plastic limit pressure for plane-strain axi-symmetric vessels in a form with an integral term as

$$\begin{aligned} \frac{q^*}{\sigma_0} &= \frac{1}{2}\sqrt{\frac{(P+R)(R+1)}{R(P+R+1)}} \\ &\quad\times \left(\frac{\sigma_\infty}{\sigma_0}\ln\frac{b^2}{a^2} - 2(\sigma_\infty/\sigma_0-1)\int_a^b \frac{(a_0^2-a^2+r^2)^{\hat{h}}}{r^{2\hat{h}+1}}\, dr\right) \end{aligned} \tag{39}$$

Note that the integral term in Eq. (39) can be solved numerically without difficulties by some computing tools, e.g. MATLAB [29].

If we consider $h=\hat{h}=0$ or $\sigma_0=\sigma_\infty$, Eq. (39) will then reduce to the value of plastic limit pressure for perfectly plastic materials as

$$\frac{q^*}{\sigma_0} = \frac{1}{2}\sqrt{\frac{(P+R)(R+1)}{R(P+R+1)}}\ln\frac{b^2}{a^2} \tag{40}$$

Furthermore, if we deal with plastically isotropic materials then we have the plastic anisotropy parameters $R=P=1$ by definition. Therefore, the value of plastic limit pressure is reduced to

$$\frac{q^*}{\sigma_0} = \frac{1}{\sqrt{3}}\ln\frac{b^2}{a^2} \tag{41}$$

Moreover, we choose the hardening exponent value as

$$h = \sqrt{\frac{R(P+R+1)}{(P+R)(R+1)}} \tag{42}$$

Then we have $\hat{h}=0.5$ by Eq. (19). Obviously, we can obtain explicitly the value of plastic limit pressure from Eq. (39) for the case with $\hat{h}=0.5$ in the form as

$$\begin{aligned} \frac{q^*}{\sigma_0} &= \frac{1}{2}\sqrt{\frac{(P+R)(R+1)}{R(P+R+1)}} \\ &\quad\times \left\{\frac{\sigma_\infty}{\sigma_0}\ln\frac{a^2}{b^2} + 2(\sigma_\infty/\sigma_0-1)\left[\frac{a_0}{a}-\frac{b_0}{b}+\ln\frac{(b+b_0)}{(a+a_0)}\right]\right\} \end{aligned} \tag{43}$$

On the other hand, if we set the value of the hardening exponent as

$$h = 2\sqrt{\frac{R(P+R+1)}{(P+R)(R+1)}} \tag{44}$$

we get $\hat{h}=1$ by Eq. (19). Certainly, we can obtain explicitly the value of plastic limit pressure from Eq. (39) corresponding to the case with $\hat{h}=1$:

$$\begin{aligned} \frac{q^*}{\sigma_0} &= \frac{1}{2}\sqrt{\frac{(P+R)(R+1)}{R(P+R+1)}} \\ &\quad\times \left[\ln\frac{a^2}{b^2} + (\sigma_\infty/\sigma_0-1)\left(\frac{a_0^2}{a^2}-\frac{b_0^2}{b^2}\right)\right] \end{aligned} \tag{45}$$

Further, the hardening exponent $h=\sqrt{3}$ corresponds to $\hat{h}=1$ for plastically isotropic materials by Eq. (44). Therefore, Eq. (45) reduces to the value of plastic limit pressure for plastically

isotropic materials with $h=\sqrt{3}$ as derived in the previous work [14]:

$$\frac{q^*}{\sigma_0}=\frac{1}{\sqrt{3}}\left[\ln\frac{a^2}{b^2}+(\sigma_\infty/\sigma_0-1)\left(\frac{a_0^2}{a^2}-\frac{b_0^2}{b^2}\right)\right] \tag{46}$$

Certainly, we can acquire explicitly the value of plastic limit pressure corresponding to some other values of the hardening exponent of the Voce hardening law [5].

5. Comparisons and validations

This paper has developed exact solutions of plastic limit pressure by utilizing both static and kinematic theorems of limit analysis for plastically orthotropic pressure vessels with strain hardening. Further, closed-form solutions have been acquired for some hardening exponent values of the Voce hardening law [5]. To illustrate the applicability of the exact solution Eq. (39) for any value of the hardening exponent, this paper applied the computing tool MATLAB [29] to numerically solve the integral term of the exact solution Eq. (39) using recursive adaptive Simpson quadrature. On the other hand, the elastic–plastic capability of the commercial finite-element code ABAQUS [30] is also employed for rigorous validations of analytical solutions.

In the following case studies, the yield strength ratio $\sigma_\infty/\sigma_0=3.0$ is adopted. For elastic–plastic analysis by ABAQUS [30], additional elastic–plastic properties are assumed such as Young's modulus $E=207$ GPa, Poisson's ratio $\nu=0.3$ and $\sigma_0=207$ MPa. Also, the values of stress ratios are required by ABAQUS [30] for plastically anisotropic materials. Due to axi-symmetry, only a five-degree segment of the cylindrical vessel is considered with the initial outer radius b_0 of 254 mm and the inner radius a_0 of 127 mm. As shown in Fig. 1, the finite-element mesh has 10 four-node plane-strain elements with symmetry boundary conditions imposed along boundaries. By ABAQUS [30], we employ the displacement control of the inner surface to simulate the action of pressure. The corresponding pressure is then calculated from the reaction forces associated with these prescribed radial displacements. Following the motion of the inner surface, the values of plastic limit pressure are obtained step by step while the cylinder is fully plastic sequentially.

5.1. Transverse isotropy

For a transversely isotropic case, the material is isotropic in a plane and has a different strength in the thickness direction. Without loss of generality, we may assume the stress ratio $R_{11}=1$ [3]. If the isotropic plane is in the plane $r-\theta$, then we have

$$R_{11}=R_{22}=1 \tag{47}$$

Accordingly, we also have

$$R=P=2R_{33}^2-1 \tag{48}$$

By Eq. (7), we get $0.5\le R_{33}\le\infty$ corresponding to the case with the stress ratios $R_{11}=R_{22}=1$. If we set the stress ratios $R_{11}=R_{22}=1$ and $R_{33}=0.8$, we obtain the plastic anisotropy parameters $R=0.28$ and $P=0.28$ by Eq. (48).

We conduct case studies with the plastic anisotropy parameters $R=P=0.28$ and $\hat{h}=0$, 0.5 and 1, respectively. The related exact closed-form solutions are available as derived in Eqs. (40), (43) and (45), respectively. As shown in Fig. 2, the analytical solutions and the numerical results either by MATLAB [29] or by ABAQUS [30] are all in good agreement. For perfectly plastic materials, namely $h=\hat{h}=0$, the value of plastic limit pressure keeps decreasing while the inner radius ratio a/a_0 increases as shown in Fig. 2. For the case with hardening properties $\sigma_\infty/\sigma_0=3.0$ and $\hat{h}=0.5$, the value of plastic limit pressure still keeps decreasing while the inner radius ratio a/a_0 increases during the widening process as demonstrated in Fig. 2. In other words, the weakening behavior induced by the widening deformation dominates over the strengthening phenomenon resulting from strain hardening. For the case with the hardening properties $\sigma_\infty/\sigma_0=3.0$ and $\hat{h}=1$, there exists a strengthening phenomenon as shown in Fig. 2. Namely, the cylindrical vessel is strengthened to resist increasing internal pressure due to the strain-hardening effect in the initial deformation process. After that, the value of plastic limit pressure starts to decrease while the weakening effect of widening deformation counteracts and dominates over the strengthening effect [15,16].

5.2. Planar anisotropy

In the case of planar anisotropy, the stress ratios R_{11}, R_{22} and R_{33} will all be different. We still assume the stress ratio $R_{11}=1$ without loss of generality [3]. Thus, we have the plastic anisotropy parameters

$$R=\frac{1+\frac{1}{R_{22}^2}-\frac{1}{R_{33}^2}}{1+\frac{1}{R_{33}^2}-\frac{1}{R_{22}^2}} \tag{49}$$

$$P=\frac{1+\frac{1}{R_{22}^2}-\frac{1}{R_{33}^2}}{\frac{1}{R_{22}^2}+\frac{1}{R_{33}^2}-1} \tag{50}$$

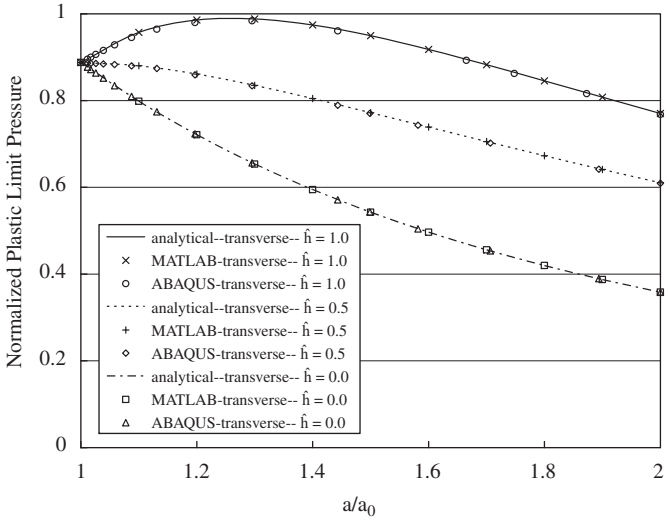

Fig. 2. Normalized plastic limit pressure P_i/σ_0 versus inner radius ratio a/a_0 for transversely isotropic materials with $\hat{h}=0$, 0.5 and 1.

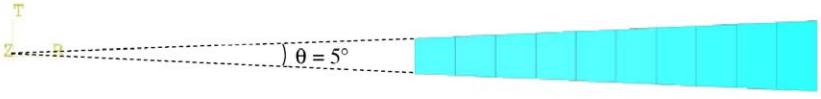

Fig. 1. Finite-element mesh for elastic–plastic analysis by ABAQUS.

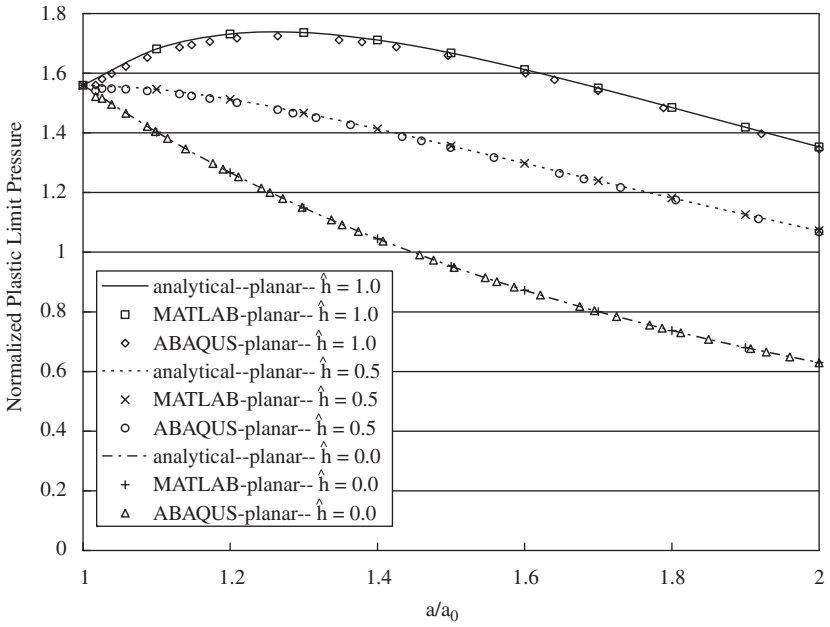

Fig. 3. Normalized plastic limit pressure P_i/σ_0 versus inner radius ratio a/a_0 for planar anisotropic materials with $\hat{h} = 0,\ 0.5$ and 1.

If we assume $R_{11} = 1$ and $R_{22} = 2.0$, then $2/3 \le R_{33} \le 2.0$ according to Eq. (7). If we consider the case with $R_{11} = 1$, $R_{22} = 2.0$ and $R_{33} = 1.5$, the corresponding plastic anisotropy parameters $R = 0.674$ and $P = -2.636$ are, respectively, determined by Eqs. (49) and (50).

The illustrated examples concerned are with the plastic anisotropy parameters $R = 0.674$ and $P = -2.636$ accompanied by $\hat{h} = 0,\ 0.5$ and 1. The corresponding exact closed-form solutions are as shown in Eqs. (40), (43) and (45), respectively. As shown in Fig. 3, there exists a good correlation between exact solutions and the numerical results either by MATLAB [29] or by ABAQUS [30]. If we consider perfectly plastic materials, namely $h = \hat{h} = 0$, the value of plastic limit pressure keeps decreasing while the inner radius ratio a/a_0 increases as shown in Fig. 3. As demonstrated in Fig. 3, there are no significant strengthening phenomena with the hardening properties $\sigma_\infty/\sigma_0 = 3.0$ and $\hat{h} = 0.5$. The value of plastic limit pressure keeps decreasing while the inner radius ratio a/a_0 increases. On the other hand, Fig. 3 also shows that the strengthening phenomenon is significant for the case with hardening properties $\sigma_\infty/\sigma_0 = 3.0$ and $\hat{h} = 1$. Apparently, we can observe that the value of plastic limit pressure increases with increasing inner radius ratio a/a_0 in the initial deformation process due to the effect of material hardening.

As pointed out previously [15,16], the variation of plastic limit pressure q^*/σ_0 with inner radius ratio a/a_0 reveals the interaction between the strengthening and weakening behavior during the expansion of strain-hardening cylindrical vessels. Further, the inner radius ratio $a/a_0 = 1$ implies the initial stage of pressurization and then there is no strain-hardening effect yet. Therefore, as shown in Figs. 2 and 3, the curves corresponding to various hardening exponent values merge together, while the inner radius ratio $a/a_0 = 1$.

6. Conclusions

In the paper, we considered cylindrical vessels under internal pressure involving the Voce hardening law and Hill's yield criterion. The widening deformation problem involving strain-hardening materials features interesting interaction between the weakening behavior induced by widening deformation and the strengthening phenomenon resulting from strain hardening. Both static and kinematic limit analysis problems were analytically studied sequentially by updating the yield strength and deformed configuration to approach the real limit solutions of plane-strain axi-symmetric vessels. Particularly, the equality relation between the greatest lower bound and the least upper bound was confirmed explicitly. Accordingly, exact solutions of plastic limit pressure with an integral term were developed for transverse isotropic and planar anisotropic materials.

As illustrated in the paper, exact closed-form solutions are available for certain values of the hardening exponent of the Voce hardening law. The applicability of the exact solution for any value of the hardening exponent of the Voce hardening law can be assured by solving the integral term of the exact solution without difficulties using some computing tools, e.g. MATLAB [29].

Numerical efforts of elastic–plastic analysis by the commercial finite-element code ABAQUS [30] were also performed for comparisons. Good agreement between analytical and numerical studies, either by MATLAB [29] or by ABAQUS [30], has demonstrated the reliability of the analytical derivations presented in the paper.

Acknowledgements

The author is deeply grateful to the referees for comments leading to substantial enhancement of the paper's quality. This research was partially supported by the National Science Council in Taiwan through Grant NSC 97-2221-E-157-007.

References

[1] Nadai A. Theory of flow and fracture of solids. New York: McGraw-Hill; 1950.
[2] Hu LW. Studies on plastic flow of anisotropic metals. J Appl Mech ASME 1956;23(3):444–50.
[3] Capsoni A, Corradi L, Vena P. Limit analysis of orthotropic structures based on Hill's yield condition. Int J Solids Struct 2001;38(22–23):3945–63.
[4] Güven U. A comparison on failure pressures of cylindrical pressure vessels. Mech Res Commun 2007;34:466–71.
[5] Voce EA. Practical strain hardening function. Metallurgia 1955;51:219–26.
[6] Huh H, Yang WH. A general algorithm for limit solutions of plane stress problems. Int J Solids Struct 1991;28(6):727–38.

[7] Jiang GL. Nonlinear finite element formulation of kinematic limit analysis. Int J Num Methods Eng 1995;38(16):2775–807.
[8] Hill R. The mathematical theory of plasticity. Oxford: Clarendon Press; 1950.
[9] Huh H, Lee CH. Eulerian finite-element modeling of the extrusion process for work-hardening materials with the extended concept of limit analysis. J Mater Process Technol 1993;38(1–2):51–61.
[10] Huh H, Lee CH, Yang WH. A general algorithm for plastic flow simulation by finite element limit analysis. Int J Solids Struct 1999;36(8):1193–207.
[11] Huh H, Kim KP, Kim HS. Collapse simulation of tubular structures using a finite element limit analysis approach and shell elements. Int J Mech Sci 2001;43(9):2171–87.
[12] Hwan CL. An upper bound finite element procedure for solving large plane strain deformation. Int J Num Methods Eng 1997;40(10):1909–22.
[13] Hwan CL. Plane strain extrusion by sequential limit analysis. Int J Mech Sci 1997;39(7):807–17.
[14] Leu SY. Convergence analysis and validation of sequential limit analysis of plane-strain problems of the von Mises model with nonlinear isotropic hardening. Int J Num Methods Eng 2005;64(3):322–34.
[15] Leu SY. Analytical and numerical investigation of strain-hardening viscoplastic thick-walled cylinders under internal pressure by using sequential limit analysis. Comput Methods Appl Mech Eng 2007;196(25–28):2713–22.
[16] Leu SY. Limit analysis of strain-hardening viscoplastic cylinders under internal pressure by using the velocity control: analytical and numerical investigation. Int J Mech Sci 2008;50(12):1578–85.
[17] Leu SY, Chen JT. Sequential limit analysis of rotating hollow cylinders of nonlinear isotropic hardening. Comput Model Eng Sci 2006;14(2):129–40.
[18] Leu SY. Investigation of rotating hollow cylinders of strain-hardening viscoplastic materials by sequential limit analysis. Comput Methods Appl Mech Eng 2008;197(51–52):4858–65.
[19] Yang WH. Large deformation of structures by sequential limit analysis. Int J Solids Struct 1993;30(7):1001–13.
[20] Corradi L, Panzeri N, Poggi C. Post-critical behavior of moderately thick axisymmetric shells: a sequential limit analysis approach. Int J Struct Stab Dyn 2001;1(3):293–311.
[21] Leu SY. Limit analysis of viscoplastic flows using an extended general algorithm sequentially: convergence analysis and validation. Comput Mech 2003;30(5–6):421–7.
[22] Corradi L, Panzeri N. A triangular finite element for sequential limit analysis of shells. Adv Eng Software 2004;35(10–11):633–43.
[23] Kim KP, Huh H. Dynamic limit analysis formulation for impact simulation of structural members. Int J Solids Struct 2006;43(21):6488–501.
[24] Yang WH. Admissibility of discontinuous solutions in mathematical models of plasticity. In: Yang WH, editor. Topics in plasticity. Michigan: AM Press; 1991. p. 241–60.
[25] Liu C, Huang Y, Stout MG. On the asymmetric yield surface of plastically orthotropic materials: a phenomenological study. Acta Mater 1997;45(6): 2397–406.
[26] Wagoner RH, Chenot J. Fundamentals of metal forming. New York: Wiley; 1996.
[27] Yang WH. On generalized Hölder inequality. Nonl Anal Theory Methods Appl 1991;16:489–98.
[28] Drucker DC. A definition of stable inelastic material in the mechanics of continua. J Appl Mech ASME 1959;81:101–6.
[29] MATLAB. MATLAB R2008a documentation. Massachusetts: The MathWorks, Inc.; 2008.
[30] ABAQUS. ABAQUS/Standard v6.5 user's manual. Rhode Island: ABAQUS Inc.; 2004.